J. Fluid Mech. (1974), *vol.* 64, *part* 4, *pp.* 701–724
Printed in Great Britain

Diffusion-flame structure for a two-step chain reaction

By WILLIAM B. BUSH
University of California, La Jolla, California 92037
AND FRANCIS E. FENDELL
TRW Systems Group, Redondo Beach, California 90278

(Received 7 May 1973 and in revised form 2 November 1973)

The low-speed combustion of initially unmixed gaseous reactants under an irreversible two-step chain reaction is examined. Both equilibrium burning, in which two spatially separated flames of zero thickness arise, and near-equilibrium burning, in which two spatially separated flames of small but finite thickness arise, are studied by limit-process expansion techniques. Two time-dependent flows are examined: the first is (one-dimensional) transient mixing flow; and the second is (two-dimensional) transient counterflow. The latter flow, in which there is an impressed finite strain parallel to the flame, such that the flame itself is longitudinally stretched, is discussed as elucidating the characteristics of combustion in non-equilibrium turbulent shear flow.

1. Introduction

Equilibrium irreversible burning of initially unmixed gaseous reactants under a direct one-step mechanism leads to a flame (mathematically) of zero thickness, situated where the reactants meet in stoichiometric proportions (Burke & Schumann 1928). There is no interpenetration of reactants, with the flame acting as a sink for reactants and a source for products. Diffusion dominates convection as the mode of mass and heat transport in the immediate vicinity of the flame, whence the name diffusion flame (Williams 1965). Slight departures from equilibrium and/or irreversibility result in a thin flame of non-zero thickness. Limit-process expansion techniques (for a Lewis number of unity) have been employed, both formally and informally, to perturb about the singular flame-sheet limit (Friedlander & Keller 1963; Liñan 1963; Pearson 1963; Fendell 1965, 1967).

Direct one-step chemical kinetics is a frequently useful phenomenological model. However, there are many chemical processes in which no one step is rate controlling, and the multi-step nature of the chemical mechanism must be explicitly examined. The special properties of the multi-step kinetics of hydrogen–oxygen combustion without premixing have been studied under the singular near-equilibrium and near-irreversible conditions, but one combustion zone has always sufficed, even when many simultaneous reactions were included (Clarke 1968,

1969; Clarke & Moss 1969). Other authors have considered different chemical mechanisms, and have suggested that spatially separated flame surfaces may be employed to model the combustion. For example, two flame surfaces have been used to describe a reversible one-step reaction in chemical equilibrium for a boundary-layer flow (Cohen, Bromberg & Lipkis 1958); however, two spatially separated flames can never be generated by a one-step reaction, and the model proposed is not a rational limit of the properly formulated boundary-value problem. Also, two separated thin flames have been used to describe the burning of a planar jet, consisting, in part, of a mixture of two chemically distinct fuels flowing into an oxygen-containing ambient atmosphere (Schetz 1970); however, oxygen does not penetrate the first thin flame under the Burke–Schumann model, and, in fact, the two thin flames have to be coincident, so that, effectively, a single fuel is being burned.

Nevertheless, there are chain-type chemical mechanisms for which, under equilibrium irreversible burning, spatially distinct diffusion flames do describe the combustion of *initially unmixed reactants*. (The so-called cool-flame phenomenon, in which spatially separated flames occur in *premixed reactants*, not necessarily owing to chain-type mechanisms, is well known (Korman 1970).) The mechanism to be examined here is the irreversible two-step chain reaction

$$A + B_2 \rightarrow B + C, \tag{1.1a}$$

$$B + A_2 \rightarrow A + C, \tag{1.1b}$$

in which the atoms A and B serve as chain carriers. Clearly, the two-step mechanism pertains when either of the two diatomic species A_2 and B_2 has not been entirely dissociated; if species A_2 (or B_2) has been entirely predissociated, then (1.1a) (or (1.1b)) alone describes the relevant one-step mechanism. Of course, some dissociation of A_2 and/or B_2 is a prerequisite to starting the chain.

Several examples of the chain reaction (1.1) are now considered. A particularly interesting example is the burning of hydrogen and a halogen (such as fluorine), so that C denotes the product hydrogen halide. [Relative to many other reactions, the frequency factors are large and the activation temperatures are small in the specific rate constants for hydrogen–halogen reactions; the reaction rates are large and comparable, so near-equilibrium treatment of both (1.1a) and (1.1b) is of prime interest.] This case is relevant to many continuous diffusion-type chemical lasers currently under development (Kerber, Emanuel & Whittier 1972). Incidentally, in practice, the direct reaction of the atomic species A and B is three-body and, therefore, at ordinary pressures, so very much slower than either (1.1a) or (1.1b) that it may be entirely omitted. Another example of a mechanism closely related to (1.1) is the burning of a general hydrocarbon gas C_nH_m (at temperatures below those at which oxides of nitrogen occur in significant amounts). According to theory (Edelman, Fortune & Weilerstein 1972), and possibly also experiment (Tsuji & Yamaoka 1971), the unpremixed burning of the hydrocarbon and oxygen involves a two-step mechanism in which the hydrocarbon reduces oxygen from carbon dioxide to form carbon monoxide

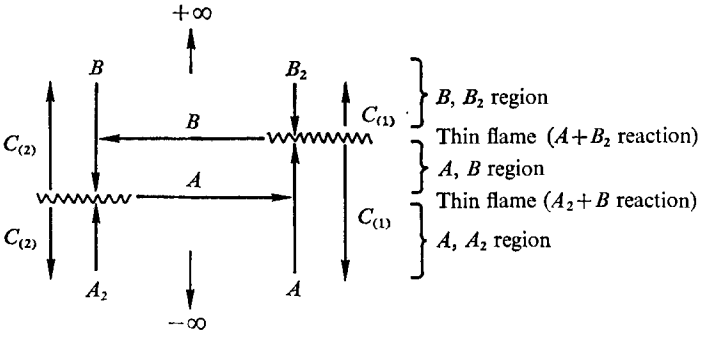

FIGURE 1. A schematic diagram of the structure of the two diffusion flames for equilibrium irreversible burning of initially unmixed species A and A_2 and B and B_2, under chemical reactions (1.1). Species A and A_2 lie to one side of the two flames; species B and B_2, to the other side. Between the two flames, only the monatomic chain carriers A and B can be found. Product species $C_{(1)}$, formed at the B_2+A flame, and $C_{(2)}$, formed at the A_2+B flame, diffuse away.

and water vapour; the monoxide burns with the oxygen to form the dioxide.† The authors report this work for completeness, without comment on its validity. A third example of a mechanism related to (1.1) is the (widely studied) two-step chain reaction for the formation of nitrogen oxide (Zeldovich 1946). In this mechanism, monatomic nitrogen (oxygen) reacts with diatomic oxygen (nitrogen) to form nitrogen oxide and monatomic oxygen (nitrogen). The analogy with (1.1) is only partial, because the reactants are premixed in many cases of interest, the reverse reactions are not negligible and the two forward rates are not comparable.

No theory describing the finite structure of multiple diffusion flames as the reaction rates are relaxed from indefinitely large values, relative to the flow rates, has been presented. Only by pursuing such corrections can the adequacy of the thin-flame limit in describing actual situations be estimated.

In this paper, two time-dependent low-speed parabolic boundary-value problems are treated (for Lewis and Prandtl numbers of unity), to elucidate the properties and structure of the two diffusion flames generated by the two-step chain (1.1*a*) and (1.1*b*) (see figure 1). The first problem is the (fundamental) transient one-dimensional mixing flow in which the convection is induced by thermal inhomogeneity. For this problem, the relative locations of the two flames in time for infinite-rate chemical kinetics are examined. The second is the

† The explicit chemical mechanisms proposed by Edelman *et al.* for unpremixed burning of the hydrocarbon gas C_nH_m in oxygen are

$$2C_nH_m + (2n+m)\,CO_2 \rightarrow (4n+m)\,CO + mH_2O,$$
$$2CO + O_2 \rightarrow 2CO_2.$$

Gurevich & Stepanov (1973) also propose a two-step mechanism for unpremixed burning of a hydrocarbon gas in oxygen, but suggest that water vapour, rather than carbon dioxide, serves as a chain carrier. From their diagrams, the mechanisms are

$$2C_nH_m + 2nH_2O \rightarrow (2n+m)\,H_2 + 2nCO,$$
$$2H_2 + O_2 \rightarrow 2H_2O.$$

The step listed first in each of these models for hydrocarbon burning is endothermic, while the step listed second is exothermic.

transient counterflow problem (cf., for example, Fendell 1967), in which forced convection, in the form of an impressed constant rate of strain along the flame, is introduced. For this problem, the location and the structure of the two flames for (large but) finite-rate chemical kinetics are studied by limit-process expansion techniques.

The solutions to both of these problems are developed from treatments of the complete time-dependent conservation laws for mass, momentum and energy in multi-component flows. Thus, solutions to these problems are relevant for laminar flows. However, recent experimental investigations (Gibson & Libby 1972; Otsuka & Niioka 1972, 1973) have argued that the second problem also furnishes insight into turbulent reacting flows of initially unmixed reactants. In fact, Klimov (1967) suggests that the second problem furnishes insight into turbulent burning of premixed reactants when reaction times are short relative to flow times. For the case of chemical kinetics involving large but finite rates, these papers suggest that turbulent reaction zones consist of thin flames stretched owing to finite tangential rates of strain. The relevance of the transient counterflow problem to turbulent reacting flow is discussed again when the solution is developed.

2. Formulation

The equations (and boundary conditions) for the two cited cases of time-dependent, two-dimensional, chemically reacting flows are formulated in this section. In this formulation, attention is focused on the following two-step irreversible chain reaction:

$$A + B_2 \overset{K_1}{\rightarrow} B + C_{(1)}, \tag{2.1a}$$

$$B + A_2 \overset{K_2}{\rightarrow} A + C_{(2)}. \tag{2.1b}$$

It is noted that $C_{(1)}$ and $C_{(2)}$ represent the chemical species AB produced by reaction 1, equation (2.1*a*), and reaction 2, equation (2.1*b*), respectively. The distinction is made here since the internal (vibrational and rotational) states of the products $C_{(1)}$ and $C_{(2)}$ may differ.

In conventional notation, for low-speed flow with Lewis and Prandtl numbers of unity and with the dynamic viscosity linearly proportional to the temperature, the non-dimensional conservation equations† are (Williams 1965; Bush & Fendell 1973*a*)

$$\rho T = 1, \tag{2.2}$$

$$\frac{\partial}{\partial t}\left(\frac{1}{T}\right) + \frac{\partial}{\partial x}\left(\frac{u}{T}\right) + \frac{\partial}{\partial y}\left(\frac{v}{T}\right) = 0, \tag{2.3}$$

† In the non-dimensionalization, a typical length is taken to be $(\rho^\dagger k_r^\dagger/\mu_r^\dagger)^{\frac{1}{2}}$, and a typical time as $k_r^\dagger$, where $k_r^\dagger$ is a typical strain rate. The quantity Y_i is the stoichiometrically adjusted mass fraction of species i, i.e., the mole fraction of species i under the approximation that the molecular weights of all species are nearly equal. Discretion is necessary when the results are applied to gaseous mixtures containing hydrogen. Each dependent variable is to be interpreted as the lowest-order term of a regular perturbation, series in integral powers of the Mach-number-like parameter Π', where $\Pi' \equiv \mu_r^\dagger k_r^\dagger/p_\infty^\dagger = \mu^\dagger k_r^\dagger/\rho_r^\dagger R^\dagger T_r^\dagger \rightarrow 0$. For example, $T'(x_j', t') = T(x_j, t) + \Pi' T^{(1)}(x_j, t) + \ldots$, where $x_j' = x_j$ and $t' = t$.

$$\frac{1}{T}\left(\frac{\partial u}{\partial t}+u\frac{\partial u}{\partial x}+v\frac{\partial u}{\partial y}\right)+\frac{\partial p}{\partial x}-\frac{\partial}{\partial y}\left(T\left\{\frac{\partial u}{\partial y}+\frac{\partial v}{\partial x}\right\}\right)-\frac{\partial}{\partial x}\left(T\left\{(2+m)\frac{\partial u}{\partial x}+m\frac{\partial v}{\partial y}\right\}\right)=0, \tag{2.4a}$$

$$\frac{1}{T}\left(\frac{\partial v}{\partial t}+u\frac{\partial v}{\partial x}+v\frac{\partial v}{\partial y}\right)+\frac{\partial p}{\partial y}-\frac{\partial}{\partial y}\left(T\left\{(2+m)\frac{\partial v}{\partial y}+m\frac{\partial u}{\partial x}\right\}\right)-\frac{\partial}{\partial x}\left(T\left\{\frac{\partial u}{\partial y}+\frac{\partial v}{\partial x}\right\}\right)=0, \tag{2.4b}$$

$$\frac{1}{T}\left(\frac{\partial \Phi_q}{\partial t}+u\frac{\partial \Phi_q}{\partial x}+v\frac{\partial \Phi_q}{\partial y}\right)-\frac{\partial}{\partial y}\left(T\frac{\partial \Phi_q}{\partial y}\right)-\frac{\partial}{\partial x}\left(T\frac{\partial \Phi_q}{\partial x}\right)=0. \tag{2.5}$$

In (2.5), the linear combinations, the (so-called) Shvab–Zeldovich functions Φ_q, are defined by

$$\Phi_A = Y_A+Y_{A_2}-Y_{B_2}, \quad \Phi_B = Y_B+Y_{B_2}-Y_{A_2}, \tag{2.6a}$$

$$\Phi_{C_{(1)}} = Y_{C_{(1)}}+Y_{B_2}, \quad \Phi_{C_{(2)}} = Y_{C_{(2)}}+Y_{A_2}, \tag{2.6b}$$

$$\Phi_T = T+Q_1'Y_{B_2}+Q_2'Y_{A_2}. \tag{2.6c}$$

With the introduction of the differential operator L, defined by

$$L\{f_n(x_j;t)\} = \left\{\frac{1}{T}\left(\frac{\partial}{\partial t}+u\frac{\partial}{\partial x}+v\frac{\partial}{\partial y}\right)-\frac{\partial}{\partial y}\left(T\frac{\partial}{\partial y}\right)-\frac{\partial}{\partial x}\left(T\frac{\partial}{\partial x}\right)\right\}f_n(x,y,t), \tag{2.7}$$

the equations (2.5) for the Shvab–Zeldovich functions may be re-expressed as

$$L\{\Phi_q\} = 0. \tag{2.8}$$

In general, species continuity and/or energy equations must complement (2.2)–(2.5) so that each chemical reaction rate appears explicitly. In the notation of (2.7), the species continuity and energy equations are given by [Ω_1' and Ω_2' are the (so-called) first Damköhler numbers]

$$\left.\begin{aligned} L\{Y_A\} &= -\Omega_1'\Upsilon_1+\Omega_2'\Upsilon_2, \quad L\{Y_{A_2}\} = -\Omega_2'\Upsilon_2, \\ L\{Y_B\} &= \Omega_1'\Upsilon_1-\Omega_2'\Upsilon_2, \quad L(Y_{B_2}\} = -\Omega_1'\Upsilon_1, \\ L\{Y_{C_{(1)}}\} &= \Omega_1'\Upsilon_1, \quad L\{Y_{C_{(2)}}\} = \Omega_2'\Upsilon_2, \end{aligned}\right\} \tag{2.9a}$$

$$L\{T\} = \Omega_1'Q_1'\Upsilon_1+\Omega_2'Q_2'\Upsilon_2, \tag{2.9b}$$

with

$$\Upsilon_1 = T^{-1}\exp\{-\theta_1'(T_1'^*-T)/T\}Y_AY_{B_2}, \tag{2.10a}$$

$$\Upsilon_2 = T^{-1}\exp\{-\theta_2'(T_2'^*-T)/T\}Y_BY_{A_2}. \tag{2.10b}$$

The quantities Q_k' are non-dimensionalized heats of reaction. The quantities $T_k'^*$ arise because factors characterizing the Arrhenius exponential function have been incorporated in the first Damköhler numbers Ω_k'. In succeeding sections, attention is directed to the case of rapid-rate (near-equilibrium) chemical kinetics, for which $\Omega_k' \to \infty$, while $\theta_k' \to O(1)$. For now, it is emphasized that, for cases of interest, the ratios θ_1'/θ_2' and Ω_1'/Ω_2' are $O(1)$.

The above equations are supplemented by boundary and initial conditions (to be specified) that are compatible with the given flow situations. Here, it is noted that, for the two flows considered, the flow fields are spatially unbounded with initially unmixed reactants such that, as $y \to \infty$, there is a reservoir of species B and/or B_2 (say), with neither A nor A_2 present, and, as $y \to -\infty$, there is a reservoir of species A and/or A_2, with neither B nor B_2 present.

3. The one-dimensional transient mixing flow case

The first flow geometry considered is the (fundamental) one-dimensional transient mixing flow (with no impressed rate of strain). An analysis of this flow is presented for the equilibrium reaction case, with $\Omega_k'^{-1} = 0$. This analysis develops results concerning the behaviour of the flow exterior to the (two spatially separated) flame fronts, which are applied (in § 4) to the second flow geometry for the near-equilibrium reaction case, with $\Omega_k'^{-1} \to 0$.

For the mixing flow case, the flow quantities are taken to be

$$\left.\begin{aligned} u(x,y,t) &\equiv 0, \qquad v(x,y,t) = V(y,t), \qquad p(x,y,t) = P(y,t), \\ T(x,y,t) &= H(y,t), \quad Y_i(x,y,t) = J_i(y,t), \quad \Phi_q(x,y,t) = F_q(y,t). \end{aligned}\right\} \tag{3.1}$$

The resulting reduced equations for this flow are

$$\frac{\partial}{\partial t}\left(\frac{1}{H}\right) + \frac{\partial}{\partial y}\left(\frac{V}{H}\right) = 0, \tag{3.2a}$$

$$\frac{1}{H}\left(\frac{\partial V}{\partial t} + V\frac{\partial V}{\partial y}\right) + \frac{\partial P}{\partial y} - (2+m)\frac{\partial}{\partial y}\left(H\frac{\partial V}{\partial y}\right) = 0, \tag{3.2b}$$

$$\frac{1}{H}\left(\frac{\partial F_q}{\partial t} + V\frac{\partial F_q}{\partial y}\right) - \frac{\partial}{\partial y}\left(H\frac{\partial F_q}{\partial y}\right) = 0. \tag{3.2c}$$

Application of a modified Howarth–Dorodnitsyn transformation (cf., for example, Stewartson 1964, chap. 6) $(y,t) \to (\zeta,\tau)$, with

$$\tau = t, \quad \zeta = \int_0^y \frac{dz}{H}, \tag{3.3a}$$

to (3.2*a*) yields

$$V' = \frac{\partial}{\partial \tau}\left(\int_0^\zeta H'\,d\chi\right) + \Psi_0' H' = \frac{\partial}{\partial \tau}\left(\int_0^\zeta H'\,d\chi\right) \quad \text{for} \quad V' \to 0 \text{ as } \zeta \to 0, \tag{3.3b}$$

with $V'(\zeta,\tau) = V(y,t)$, $H'(\zeta,\tau) = H(y,t)$ and $\Psi_0'(\tau) \equiv 0$. Under this transformation, then, it is seen from (3.2*c*) that the functions $F_q'(\zeta,\tau) = F_q(y,t)$ satisfy, in the domain $\tau > 0$, $-\infty < \zeta < \infty$,

$$\partial F_q'/\partial\tau - \partial^2 F_q'/\partial\zeta^2 = 0, \tag{3.4}$$

the (so-called) diffusion equation.

Associated with equations (3.4) are the following initial conditions:

$$F_q'(\zeta,0) = F_q'^0(\zeta), \quad \text{a specified function;} \tag{3.5a}$$

$$F_q'^0(+\infty) = \hat{F}_q, \quad \text{a constant;} \quad F_q'^0(-\infty) = \check{F}_q, \quad \text{a constant.} \tag{3.5b}$$

It is noted that, since the flow field is spatially unbounded with initially unmixed reactants, as $\zeta \to +\infty$, there is a reservoir of species B and/or B_2 (say), but none of species A or A_2 or (for the case of interest here) C is present; while, as $\zeta \to -\infty$, there is a reservoir of species A and/or A_2, but none of species B or B_2 or (for the case of interest here) C is present. Thus,

$$\hat{F}_A = -\hat{J}_{B_2}, \quad \hat{F}_B = \hat{J}_B + \hat{J}_{B_2}, \quad \hat{F}_{C_{(1)}} = \hat{J}_{B_2}, \quad \hat{F}_{C_{(2)}} = 0, \quad \hat{F}_T = \hat{H} + Q_1'\hat{J}_{B_2}; \tag{3.6a}$$

$$\check{F}_A = \check{J}_A + \check{J}_{A_2}, \quad \check{F}_B = -\check{J}_{A_2}, \quad \check{F}_{C_{(1)}} = 0, \quad \check{F}_{C_{(2)}} = \check{J}_{A_2}, \quad \check{F}_T = \check{H} + Q_2'\check{J}_{A_2}. \tag{3.6b}$$

For the case of chemical equilibrium, i.e. $\Omega_k'^{-1} = 0$, (3.4) and (3.5) must be supplemented by additional information concerning the behaviour of the components of the functions F_q' at the reaction fronts $\zeta_k(\tau)$. Here, $\zeta_1(\tau)$ and $\zeta_2(\tau)$ denote the (to be determined) locations at time τ of the (so-called) thin flames for reactions 1 and 2, respectively. With $\Omega_k'^{-1} = 0$, for preservation of finite transport of heat and mass, it is necessary that, for all ζ,

$$\Upsilon_1 = H'^{-1}\exp\{-\theta_1'(T_1'^* - H')/H'\}J_A'J_{B_2}' = 0, \quad \text{so that} \quad J_A'J_{B_2}' = 0; \quad (3.7a)$$

$$\Upsilon_2 = H'^{-1}\exp\{-\theta_2'(T_2'^* - H')/H'\}J_B'J_{A_2}' = 0, \quad \text{so that} \quad J_B'J_{A_2}' = 0. \quad (3.7b)$$

On the physical grounds that the minimum discontinuity is preferred (i.e. the components of the functions F_q' should be continuous at the reaction fronts, but not necessarily the gradients of the components), Burke & Schumann (1928) suggested that, for $\Omega_k'^{-1} = 0$, reactions 1 and 2, respectively, are confined to the interface $\zeta_1(\tau)$ and $\zeta_2(\tau)$, (mathematically) of zero thickness, where the reactants meet in stoichiometric proportions. Then,

$$J_A', J_{B_2}' \to 0 \quad \text{as} \quad \zeta \to \zeta_1; \qquad J_B', J_{A_2}' \to 0 \quad \text{as} \quad \zeta \to \zeta_2. \qquad (3.8a, b)$$

Equations (2.1) *and* (3.8) *are compatible if and only if* $\zeta_1(\tau) \geqslant \zeta_2(\tau)$. Equation (3.4), written for each of the five functions F_q', subject to the requirements of (3.7), yields seven equations for the seven variables H' and J_i'.

The solutions of (3.4) and (3.5) (cf., for example, Carslaw & Jaeger 1959, p. 53) are represented by

$$F_q'(\zeta, \tau) = \frac{1}{(4\pi\tau)^{\frac{1}{2}}}\int_{-\infty}^{\infty} F_q'^{(0)}(\chi)\exp\left\{-\frac{(\zeta-\chi)^2}{4\tau}\right\}d\chi. \qquad (3.9)$$

Further details and numerical results for the solutions for specific (including non-self-similar) examples are presented in appendix A.

The solution of these problems indicates that the two-step symmetrical chain reaction posed by (2.1) does, under equilibrium irreversible conditions in which fuel and oxidant species are initially unmixed, lead to two spatially separated thin flames with only the monatomic chain-carrying species present between the flames (see figure 1). Furthermore, with the depletion of either of the diatomic species, the chemical reaction involving that diatomic species goes to extinction (so that the more commonly treated case of a single diffusion flame evolves). Extinction may be suggested within the context of the thin-flame solution by rapid translation of the flame to the flow boundaries, or movement off to infinity in an unbounded geometry.

Departure from equilibrium irreversible conditions in diffusion-flame burning may arise, of course, because of physical phenomena other than depletion of a reactant. For example, the first Damköhler number may tend to order unity as the characteristic flow time becomes comparable with the characteristic reaction time. A transient counterflow, in which the inverse of the local strain rate furnishes the characteristic flow time, is considered in the next section. If the chemical kinetics are such that the rates of reaction for (2.1*a*) and (2.1*b*) are comparable, and if the strain rate does not have very large spatial gradients, then a large strain rate would imply that both reactions simultaneously pass from thin-flame conditions; this contrasts with reactant-depletion considerations in which, as noted, only one reaction might pass from thin-flame conditions.

4. The transient counterflow case

The steady counterflow geometry, in which two directly opposed continuous streams meet, mix and flow laterally away, has become, both theoretically and experimentally, a frequently adopted geometry for studying properties of laminar diffusion flames (Fendell 1965, 1967; Tsuji & Yamaoka 1971; Otsuka & Niioka 1972, 1973). Here, the *time-dependent* counterflow is examined for the initially unmixed burning of fuel and oxidant for the two-step chain reaction of (2.1). Brief allusion has been made in § 1 to the fact that the motivation for considering such a flow stems from recently observed properties of transitional and non-equilibrium free turbulent flows. It is pertinent to consider this motivation in further detail at this point.†

4.1. *Motivation relative to turbulent reacting flow*

Progress in turbulent reacting flows has lagged behind that in laminar reacting flows. The traditional approach to the study of turbulent reacting flows has been to apply (Reynolds) time averaging to the conservation laws, the closure of the resulting set of equations requiring the identification of the time averages of fluctuating quantities (introduced by the nonlinear inertial transport terms *and* by the nonlinear reaction-rate terms in the law of mass action) in terms of mean field quantities. It is uncertain that universally applicable closures can be formulated; but it is certain that current empirical guidance for formulating even tentative closures is so lacking that such an approach is currently very speculative.

One apparent alternative is to try to extract helpful insight from equations that one is certain do apply to turbulent reacting flow, namely, the time-dependent conservation laws. The following discussion represents an effort in this direction for unpremixed burning in the near-equilibrium limit.

Consider mixing in a two-dimensional free shear layer downstream of a splitter plate separating initially unmixed reactants. If the fluid were to have zero coefficient of diffusion for mass, then an interface, commencing at the splitter plate and extending downstream, could be defined which separates the reactants. For turbulent flow, this interface might become more and more highly convoluted, and even multiply connected, but it would remain intact indefinitely far downstream. The velocity vector should be locally and transiently parallel to the interface, because there is no flow across the interface. If the coefficient of diffusion were now taken to be small but finite, there would be slight interpenetration of the two species in the vicinity of the interface. Furthermore, if the two species were highly reactive, then the thin flame would have to lie in the region where the reactants coexist, i.e. in the limited region of interdiffusion in the vicinity of the interface. The flow in the region of interdiffusion would have large tangential shear stresses.

The reason why, for a given distance downstream from the end of a splitter

† The authors wish to acknowledge discussions on this subject with Prof. Frank E. Marble of the California Institute of Technology.

plate, a turbulent flow consumes more reactant than a laminar flow is that the highly convoluted turbulent flame is so much longer per unit streamwise distance. There is also the possibility that the spatially and temporally changing velocity along the flame may alter the rate of reactant consumption at the flame, i.e. not only is the flame in the turbulent case longer than in the laminar case, but also the pronounced rate of strain along the flame may affect the burning rate per unit flame length. While strain along the flame would result in net stretching, indefinite lengthening cannot occur because inevitably a narrow protuberance of one reactant into the bulk of the other must result, and such extrusions would be burned off to leave an effectively shortened flame. If the rates of consumption of the reactants over a region of turbulent shear flow with unpremixed burning appear quasi-steady, then such counteracting effects are in approximate balance.

There are, of course, aspects of the speculations of the last two paragraphs that require further discussion. For example, the thickness of the region of interdiffusion, in which molecular diffusion instantaneously acts, is proposed to be appreciably smaller than the mean thickness of the mixing layer itself. It is a matter of conjecture as to just how thin this laminar interdiffusion region is relative to the mean thickness of the layer, and, quantitatively, the resolution of this point awaits additional experimental measurements. Furthermore, the interdiffusion region may well be a distinguishable zone of the mean mixing-layer thickness in transitional flow (where laminar instability and vortex pairing are first observed), and probably in non-equilibrium turbulent flow in a free mixing layer as well. At present, whether or not the interface becomes so convoluted downstream that the structure discussed here becomes eventually indiscernible does not seem to be fully resolved. Wherever the concept of a discernible interdiffusion region within the significantly thicker mean mixing layer is valid, the mean and instantaneous profiles for the mass fractions and enthalpy may differ appreciably. Under such circumstances the probability distribution functions for the fluctuating components of these dependent variables are highly non-Gaussian (Bush & Fendell 1973*b*).

Experimental evidence in the literature pertinent to the structure of the mixing layer just discussed is now briefly reviewed.

Brown & Roshko (1971) have made density traverses, and taken shadowgraphs, of the fully developed, two-dimensional, chemically inert, turbulent, subsonic mixing layer downstream of a plate separating streams of appreciably different molecular weight. These workers discovered a large-scale structure on the shadowgraphs, of the thickness of the shear layer itself. Furthermore, the instantaneous density traverses revealed rather rapid transitions from the lighter density to the heavier density, but limited evidence of intermediate density; the time-averaged traverses revealed the conventional equilibrium turbulent shear-layer profile for the mean density. These results seem to suggest the existence of a narrow interface between the species with little interpenetration, the large-scale structure permitting gas from one side of the layer to be convected to the other side. The existence of such a large-scale structure is clearly lost in the time averaging. The large-scale structure may be identified with the interface discussed above. Grant, Jones & Rosenfeld (1973) have since reported

shadowgraphs of turbulent diffusion flames involving axisymmetric jets of propane issuing into a stagnant atmosphere. These shadowgraphs confirm the existence of a large-scale orderly structure, and the persistence of discrete regions of fuel and oxident well into the burning region.

Gibson & Libby (1972) noticed the possible existence of narrow sharply defined reaction zones in their probings of an unpremixed acid–base reaction in a turbulent flow. The existence of such thin reaction zones contradicts the concept of instantaneously spatially diffuse burning in a turbulent diffusion flame, although a diffuse flame results on time averaging (Hawthorne, Weddel & Hottel 1949). Gibson & Libby note the importance of finite strain along the flame, but furnish no study of a flame with a parallel impressed strain rate for the transient case pertinent to gases. Such a solution is given in appendix B.

Otsuka & Niioka (1972) note that, experimentally, for the two-dimensional diffusion flame with a longitudinal strain such that the flame is stretched, there is, in general, a deviation between the flame location and the stagnation plane of the flow. Results in appendix B confirm this observation. These authors also note a departure from the thin-flame results when the rate of strain becomes too large. It has already been noted that increasing the strain rate, while holding all other parameters fixed, eventually will result in departure from the interfacial combustion where the reactants meet in stoichiometric proportions.

Thus, experimental and theoretical work on unpremixed combustion in free turbulent shear layers suggests that the burning occurs instantaneously along highly convoluted thin interfaces, continually stretched and lengthened by a longitudinal strain. Only upon time averaging would the rapidly translating, relatively thin combustion interfaces yield spatially distributed combustion zones. Furthermore, this work suggests that a close-up view of processes occurring in the immediate vicinity of the thin flame is furnished by the transient counterflow case with a finite time-dependent longitudinal strain rate.

4.2. *Interpretation of the solution*

The solution to the transient counterflow problem, in which there is a time-invariant reservoir of species A and A_2 as $y \to -\infty$, and of species B and B_2 as $y \to +\infty$, these species chemically reacting according to (2.1), is given in appendix B. Here some physically noteworthy aspects of the solution are discussed.

A solution exists to the conservation equations (2.2)–(2.10) in which the normal velocity v, temperature T and concentrations Y_i are functions of (y, t) only, while the tangential velocity $u = x/(t+t_0)$, where t_0 is a reference time. Thus, the solution does indeed describe a case in which there is a spatially constant, though temporally varying, strain rate tangential to any flames that arise. The thin flames that do arise in the (self-similar) *equilibrium irreversible case* are two spatially separated flames entirely consistent with figure 1. Because of the insight gained from § 3, little further discussion of this case is required. It is noted, however, that the flames spatially approach one another when the ambient concentrations of both of the monatomic species A and B tend to zero.

Further, the rates of consumption increase as the square root of the strain rate, when all other parameters are held fixed; the tangential straining induces an influx of fresh reactants to the burning interfaces to augment the rate of product creation.

Too large straining, however, can cause *departures from chemical equilibrium*, and thus possible reduction in consumption rates. For small departures from chemical equilibrium, for the second-order reactions given in (2.1), the non-self-similar corrections to the equilibrium irreversible solutions are exponentially small in magnitude, except in regions $O(\Omega_k'^{-\frac{1}{3}})$ in thickness about the thin-flame positions, where Ω_k' is the appropriate characterization of the first Damköhler number for the parameter expansion analysis (see next paragraph). This statement implies that, for example, only an exponentially small amount of species A passes through the upper flame (see figure 1) unreacted to the predominantly B_2 side of the burning zone. The two flames possess small though finite structure, and in general do not interact. Thus, for example, in the upper burning region, in which $O(\Omega_k'^{-\frac{1}{3}})$ amounts of A and B_2 coexist, and in which the maximum enthalpy is decreased by an amount of $O(\Omega_k'^{-\frac{1}{3}})$ from its thin-flame value, diffusion and chemical reaction are the dominant physical processes; convection enters first in the next higher order of approximation for the burning zone.

Departures from equilibrium irreversible conditions decrease when the strain rate becomes small relative to the reaction rate. Since the tangential strain rate is inversely proportional to time t, under the boundary–initial conditions considered here, the thin-flame solution is approached sooner for larger reaction rates (parameter expansion analysis), but is eventually approached for long times by all finite reaction rates (co-ordinate expansion analysis). Interestingly, the spatial extent of the region in which there is an algebraically large departure from thin-flame conditions increases as $t^{\frac{1}{3}}$, but the magnitudes of the departures from the thin-flame values decrease as $t^{-\frac{1}{2}}$.

The authors are very grateful to Dr J. E. Broadwell of TRW Systems, Redondo Beach, California; Prof. F. E. Marble of the California Institute of Technology, Pasadena, California; and to Prof. F. A. Williams of the University of California, San Diego, La Jolla, California, for helpful discussions and encouragement. This work was sponsored by Project SQUID, which is supported by the Office of Naval Research, Department of the Navy, under contract N00014-67-A-0226-0005, NR-098-038. Reproduction in part or in full is permitted for any use of the United States Government.

Appendix A. The one-dimensional transient mixing flow case

Consider the specific example where the initial conditions for the variables $H'(\zeta, 0) = H'^0(\zeta)$ and $J_i'(\zeta, 0) = J_i'^0(\zeta)$ (compatible with the boundary conditions for these variables $H'(+\infty, \tau) = \hat{H}(\tau) =$ constant, $J_i'(+\infty, \tau) = \hat{J}_i(\tau) =$ constant, $H'(-\infty, \tau) = \check{H}(\tau) =$ constant, $J_i'(-\infty, \tau) = \check{J}_i(\tau) =$ constant) are given by (cf.

§ 3 for notation)

$$H'^0 = \hat{H} = \text{constant} \quad \text{for} \quad \zeta > 0, \qquad H'^0 = \check{H} = \text{constant} \quad \text{for} \quad \zeta < 0; \tag{A 1}$$

$$J'^0_{C_{(1)}} = \hat{J}_{C_{(1)}} = 0 \quad \text{for} \quad \zeta > 0, \qquad J'^0_{C_{(1)}} = \check{J}_{C_{(1)}} = 0 \quad \text{for} \quad \zeta < 0, \tag{A 2a}$$

$$J'^0_{C_{(2)}} = \hat{J}_{C_{(2)}} = 0 \quad \text{for} \quad \zeta > 0, \qquad J'^0_{C_{(2)}} = \check{J}_{C_{(2)}} = 0 \quad \text{for} \quad \zeta < 0; \tag{A 2b}$$

$$J'^0_A = \hat{J}_A = 0 \quad \text{for} \quad \zeta > 0, \qquad J'^0_A = \check{J}_A = 0 \quad \text{for} \quad \zeta < 0, \tag{A 3a}$$

$$J'^0_{A_2} = \hat{J}_{A_2} = 0 \quad \text{for} \quad \zeta > 0, \qquad J'^0_{A_2} = \check{J}_{A_2} = \text{constant} \quad \text{for} \quad \zeta < 0; \tag{A 3b}$$

$$\left.\begin{aligned} J'^0_B = \hat{J}_B = \text{constant} \quad \text{for} \quad a < \zeta, \qquad J'^0_B = J^+_B = 0 \quad \text{for} \quad 0 < \zeta < a, \\ J'^0_B = \check{J}_B = 0 \quad \text{for} \quad \zeta < 0, \end{aligned}\right\} \tag{A 4a}$$

$$\left.\begin{aligned} J'^0_{B_2} = \hat{J}_{B_2} = 0 \quad \text{for} \quad a < \zeta, \qquad J'^0_{B_2} = J^+_{B_2} = \text{constant} \quad \text{for} \quad 0 < \zeta < a, \\ J'^0_{B_2} = \check{J}_{B_2} = 0 \quad \text{for} \quad \zeta < 0. \end{aligned}\right\} \tag{A 4b}$$

Physically, the above initial conditions model the situation where there is an impermeable non-conducting diaphragm located at $\zeta = 0$ (to be burst at time $\tau = 0$), which initially separates the fuel (species A and A_2) in the lower half-plane $\zeta < 0$ from the oxidant (species B and B_2) in the upper half-plane $\zeta > 0$. The (product-free) fuel is maintained at a constant temperature $H'^0 = \check{H}$, while the (product-free) oxidant is maintained at a constant temperature $H'^0 = \hat{H}$. It is assumed, since this is the physically interesting case, that the initial fuel temperature $\check{H}$ is less than that required for the dissociation of the fuel from its diatomic form to its monatomic form, hence $J'^0_A = 0$ and $\check{J}^0_{A_2} = \text{constant}$ for $\zeta < 0$. On the other hand, it is assumed that the initial oxidant temperature $\hat{H}$ is sufficiently higher than that required for the dissociation of the oxidant from its diatomic form to its monatomic form. Further, it is assumed that the diaphragm is very catalytic to the recombination of the oxidant from its monatomic to its diatomic form. These competing effects, thermal dissociation and catalytic recombination, in the upper half-plane are modelled by the initial conditions $J'^0_B = 0$ and $J'^0_{B_2} = J^+_{B_2} = \text{constant}$ for $0 < \zeta < a$, and $J'^0_B = \hat{J}_B = \text{constant}$ and $J'^0_{B_2} = 0$ for $a < \zeta$, with a the effective thickness of the recombination zone. The situation considered does, in fact, simulate actual circumstances in some existing hydrogen–fluorine diffusion-type chemical lasers, when the fuel is identified as hydrogen and the oxidant is identified as fluorine.

The initial conditions for the Shvab–Zeldovich functions $F'_q(\zeta, 0) = F'^0_q(\zeta)$, derived from (A 1)–(A 4), are given by

$$F'^0_A = J'^0_A + J'^0_{A_2} - J'^0_{B_2} = \left\{\begin{array}{ll} 0 & (a < \zeta), \\ -J^+_{B_2} & (0 < \zeta < a), \\ \check{J}_{A_2} & (\zeta < 0); \end{array}\right\} \tag{A 5a}$$

$$F'^0_B = J'^0_B + J'^0_{B_2} - J'^0_{A_2} = \left\{\begin{array}{ll} \hat{J}_B & (a < \zeta), \\ J^+_{B_2} & (0 < \zeta < a), \\ -\check{J}_{A_2} & (\zeta < 0); \end{array}\right\} \tag{A 5b}$$

$$F'^0_{C_{(1)}} = J'^0_{C_{(1)}} + J'^0_{B_2} = \left\{\begin{array}{ll} 0 & (a < \zeta), \\ J^+_{B_2} & (0 < \zeta < a), \\ 0 & (\zeta < 0); \end{array}\right\} \tag{A 5c}$$

$$F'^0_{C_{(2)}} = J'^0_{C_{(2)}} + J'^0_{A_2} = \begin{cases} 0 & (a < \zeta), \\ 0 & (0 < \zeta < a), \\ \check{J}_{A_2} & (\zeta < 0); \end{cases} \tag{A 5d}$$

$$F'^0_T = H'^0 + Q'_1 J'^0_{B_2} + Q'_2 J'^0_{A_2} = \begin{cases} \hat{H} & (a < \zeta), \\ \hat{H} + Q'_1 J^+_{B_2} & (0 < \zeta < a), \\ \check{H} + Q'_2 \check{J}_{A_2} & (\zeta < 0). \end{cases} \tag{A 5e}$$

Substitution of the initial values $F'^0_q(\zeta)$, for the example under consideration, into the integral representations for the solutions (3.9)

$$F'_q(\zeta, \tau) = \frac{1}{(4\pi\tau)^{\frac{1}{2}}} \int_{-\infty}^{\infty} F'^0_q(\chi) \exp\left\{-\frac{(\zeta-\chi)^2}{4\tau}\right\} d\chi \tag{A 6}$$

yields

$$F'_T = \tfrac{1}{2}[\hat{H}\{1+\operatorname{erf}\phi\} + \check{H}\{1-\operatorname{erf}\phi\} + Q'_1 J^+_{B_2}\{\operatorname{erf}\phi - \operatorname{erf}(\phi-\epsilon)\} + Q'_2 \check{J}_{A_2}\{1-\operatorname{erf}\phi\}], \tag{A 7a}$$

$$F'_A = \tfrac{1}{2}[-J^+_{B_2}\{\operatorname{erf}\phi - \operatorname{erf}(\phi-\epsilon)\} + \check{J}_{A_2}\{1-\operatorname{erf}\phi\}], \tag{A 7b}$$

$$F'_B = \tfrac{1}{2}[\hat{J}_B\{1+\operatorname{erf}(\phi-\epsilon)\} + J^+_{B_2}\{\operatorname{erf}\phi - \operatorname{erf}(\phi-\epsilon)\} - \check{J}_{A_2}\{1-\operatorname{erf}\phi\}], \tag{A 7c}$$

$$F'_{C_{(1)}} = \tfrac{1}{2}[J^+_{B_2}\{\operatorname{erf}\phi - \operatorname{erf}(\phi-\epsilon)\}], \tag{A 7d}$$

$$F'_{C_{(2)}} = \tfrac{1}{2}[\check{J}_{A_2}\{1-\operatorname{erf}\phi\}], \tag{A 7e}$$

where $\phi = \zeta/2\tau^{\frac{1}{2}}$ and $\epsilon = a/2\tau^{\frac{1}{2}}$. The solutions to the basic boundary-value problem in the equilibrium limit ($\Omega_k^{-1} = 0$), for the initial conditions (A 1)–(A 4), are given implicitly by (A 7), subject the flame-sheet boundary conditions (3.7). These positions are determined implicitly from the relations

$$\begin{aligned} F'_A &= J'_A + J'_{A_2} - J'_{B_2} \\ &\to \tfrac{1}{2}[\check{J}_{A_2} - (\check{J}_{A_2} + J^+_{B_2}) \operatorname{erf}\phi_1 + J^+_{B_2} \operatorname{erf}(\phi_1 - \epsilon)] \\ &\to 0 \quad \text{as} \quad \phi \to \phi_1 = \zeta_1/2\tau^{\frac{1}{2}}, \end{aligned} \tag{A 8a}$$

$$\begin{aligned} F'_B &= J'_B + J'_{B_2} - J'_{A_2} \\ &\to \tfrac{1}{2}[(\hat{J}_B - \check{J}_{A_2}) + (J^+_{B_2} + \check{J}_{A_2}) \operatorname{erf}\phi_2 - (J^+_{B_2} - \hat{J}_B) \operatorname{erf}(\phi_2 - \epsilon)] \\ &\to 0 \quad \text{as} \quad \phi \to \phi_2 = \zeta_2/2\tau^{\frac{1}{2}}. \end{aligned} \tag{A 8b}$$

From a careful examination of (A 8*a*, *b*), it is determined that $\phi_1 \geqslant \phi_2$ and/or $\zeta_1 \geqslant \zeta_2$. It is noted that determination of $\zeta_1(\tau)$ and $\zeta_2(\tau)$ from (A 8*a*, *b*) for specific values of the parameters $\check{J}_{A_2}$, $\hat{J}_B$ and $J^+_{B_2}$ is perhaps most readily carried out by integration of

$$\frac{d\zeta_1}{d\tau} = -\left.\frac{\partial F'_A/\partial\tau}{\partial F'_A/\partial\zeta}\right|_{\zeta=\zeta_1}, \quad \frac{d\zeta_2}{d\tau} = -\left.\frac{\partial F'_B/\partial\tau}{\partial F'_B/\partial\zeta}\right|_{\zeta=\zeta_2}, \tag{A 8c}$$

with $\zeta_1, \zeta_2 \to 0$ as $\tau \to 0$. Next, it is determined that

$$F'_B \to \tfrac{1}{2}\hat{J}_B\{1+\operatorname{erf}(\phi_1-\epsilon)\} = J'^*_{B,1} \quad \text{as} \quad \phi \to \phi_1, \tag{A 9a}$$

$$F'_A \to \tfrac{1}{2}\hat{J}_B\{1+\operatorname{erf}(\phi_2-\epsilon)\} = J'^*_{A,2} \quad \text{as} \quad \phi \to \phi_2; \tag{A 9b}$$

$$F'_T \to \tfrac{1}{2}[(\hat{H}+\check{H}) + (Q'_1+Q'_2)\check{J}_{A_2}]\{1-\operatorname{erf}\phi_1\} + \hat{H}\operatorname{erf}\phi_1 = T'^*_1 \quad \text{as} \quad \phi \to \phi_1, \tag{A 10a}$$

$$F'_T \to \tfrac{1}{2}\{(\hat{H}+\check{H}) + (Q'_1+Q'_2)\check{J}_{A_2}\}\{1-\operatorname{erf}\phi_2\} + \hat{H}\operatorname{erf}\phi_2 - \tfrac{1}{2}Q'_1\hat{J}_B \times\{1+\operatorname{erf}(\phi_2-\epsilon)\} = T'^*_2 \quad \text{as} \quad \phi \to \phi_2. \tag{A 10b}$$

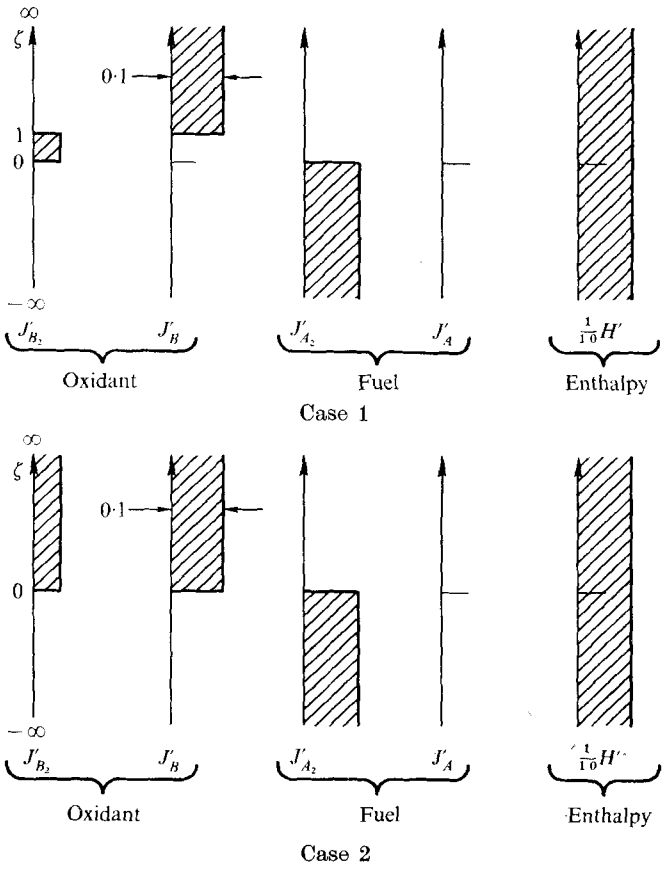

FIGURE 2. Initial profiles for the dependent variables. The evolution in time for case 1, developed in (A 1)–(A 12), is depicted in figures 3 and 4. The evolution in time for case 2, introduced in (A 13), is depicted in figures 5 and 6. For both case 1 and also case 2, there is no product gas taken to be initially present, i.e., $J'_{C_{(1)}} = J'_{C_{(2)}} = 0$ for all ζ at $\tau = 0$.

Here, the facts that $J'_{B_2} = 0$ for $\zeta \leqslant \zeta_1$ and that $J'_{A_2} = 0$ for $\zeta \geqslant \zeta_2$ have been employed.

The solutions to the boundary-value problem can now be given explicitly in terms of the Shvab–Zeldovich functions presented in (A 7). These solutions are

$$J'_A, J'_{A_2} = 0, \quad J'_B = F'_B + F'_A, \quad J'_{B_2} = -F'_A,$$
$$J'_{C_{(1)}} = F'_{C_{(1)}} + F'_A, \quad J'_{C_{(2)}} = F'_{C_{(2)}}, \quad H' = F'_T + Q'_1 F'_A \quad \text{in} \quad \zeta_1 < \zeta < \infty; \tag{A 11a}$$
$$J'_{A_2}, J'_{B_2} = 0, \quad J'_A = F'_A, \quad J'_B = F'_B,$$
$$J'_{C_{(1)}} = F'_{C_{(1)}}, \quad J'_{C_{(2)}} = F'_{C_{(2)}}, \quad H' = F'_T \quad \text{in} \quad \zeta_2 < \zeta < \zeta_1; \tag{A 11b}$$
$$J'_B, J'_{B_2} = 0, \quad J'_A = F'_A + F'_B, \quad J'_{A_2} = -F'_B,$$
$$J'_{C_{(1)}} = F'_{C_{(1)}}, \quad J'_{C_{(2)}} = F'_{C_{(2)}} + F'_B, \quad H' = F'_T + Q'_2 F'_B \quad \text{in} \quad -\infty < \zeta < \zeta_2. \tag{A 11c}$$

For aid in the presentation of the temperature and species concentration profiles for this two-flame mechanism in unpremixed burning, an illustrative

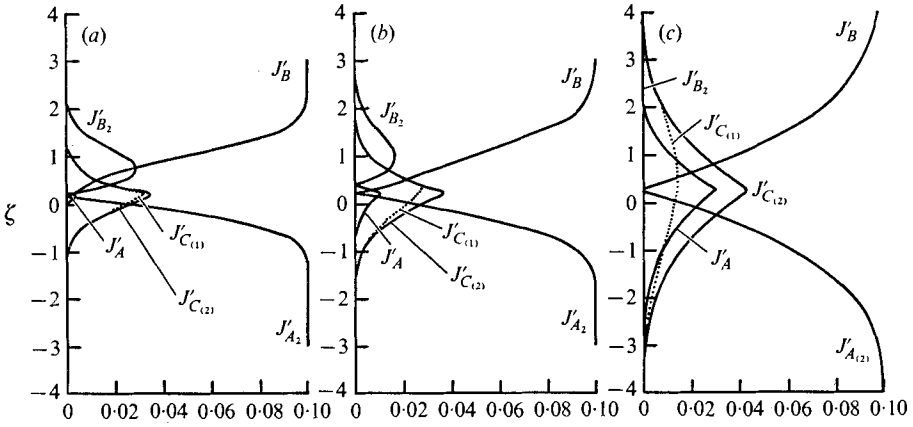

FIGURE 3. The evolution in time τ for the initial profiles given as case 1 in figure 2. For small times, two spatially separated flames develop, but by time $\tau = 1{\cdot}0$ the initial finite quantity of J'_{B_2} has been so depleted that little additional $J'_{C_{(1)}}$ is being produced. (*a*) $\tau = 0{\cdot}1$. (*b*) $\tau = 0{\cdot}2$. (*c*) $\tau = 1{\cdot}0$.

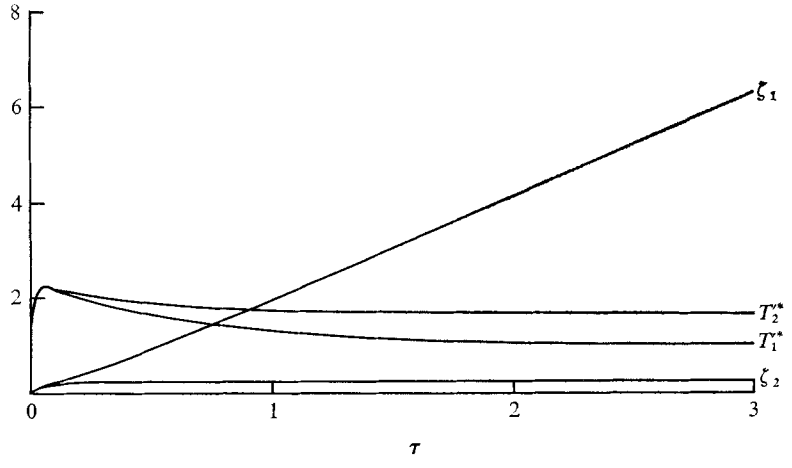

FIGURE 4. Further results depicting the evolution in time τ for case 1 of figure 2. Whereas the flame front ζ_2 (at which J'_{A_2} and J'_B pass to $J'_{C(2)}$) translates but little in time, the flame front ζ_1 (at which J'_A and J'_{B_2} pass to $J'_{C(1)}$) translates appreciably. Initially the temperature $T_1'^*$ at ζ_1 is the maximum because that reaction is more exothermic, but soon so little unburned J'_{B_2} remains that the temperature $T_2'^*$ at ζ_2 is maximum.

computation has been performed. In this computation, the parameters have the following values (pertinent to the burning of hydrogen and fluorine highly diluted in nitrogen):

$$\hat{H}, \check{H} = 1, \quad \check{J}_{A_2}, \hat{J}_B, 2J^+_{B_2} = 0{\cdot}1, \quad Q'_1 = 27{\cdot}7, \quad Q'_2 = 9{\cdot}1, \quad a = 1. \quad \text{(A 12)}$$

Results of the computation are given in figures 2–4.

A slightly modified case is obtained by reducing the temperature $H'^0 = \hat{H}$ of the fuel so that partial dissociation occurs throughout the upper half-plane (the diaphragm is now taken to be non-catalytic). In all other respects, the

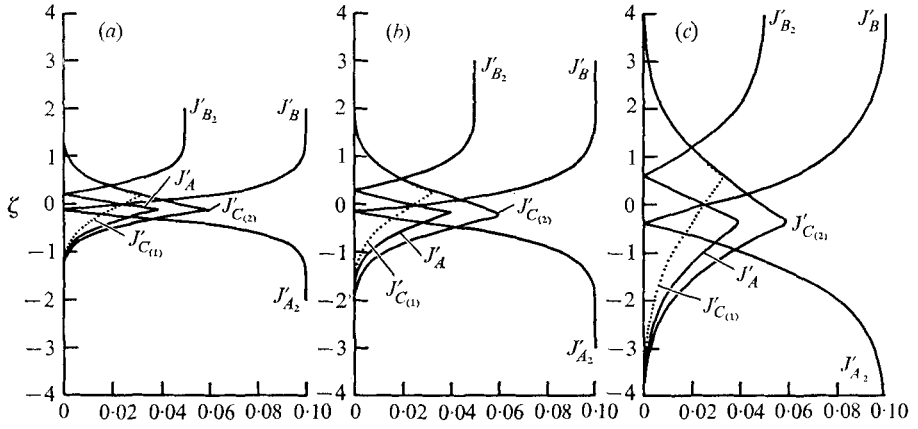

FIGURE 5. The evolution in time τ for the initial profiles given as case 2 in figure 2. Here, two spatially distinct flames develop and continue to burn vigorously. (*a*) $\tau = 0{\cdot}1$. (*b*) $\tau = 0{\cdot}2$. (*c*) $\tau = 1{\cdot}0$.

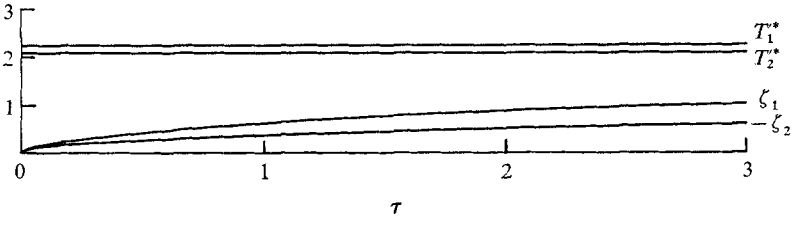

FIGURE 6. Further results depicting the evolution in time τ for case 2 of figure 2. The parabolic curves depicting the movement of the flame fronts ζ_1 and ζ_2 in time, and the constancy of the flame temperatures $T_1'^*$ at ζ_1 and $T_2'^*$ at ζ_2, reflect the self-similar character of the solution.

problem remains unchanged. The initial conditions expressed in (A 1)–(A 3) still hold, but in place of (A 4),

$$J'^0_B = \hat{J}_B = \text{constant} \quad \text{for} \quad \zeta > 0, \qquad J'^0_B = \check{J}_B = 0 \quad \text{for} \quad \zeta < 0, \quad \text{(A 13}a\text{)}$$

$$J'^0_{B_2} = \hat{J}_{B_2} = \text{constant} \quad \text{for} \quad \zeta > 0, \qquad J'^0_{B_2} = \check{J}_{B_2} = 0 \quad \text{for} \quad \zeta < 0. \quad \text{(A 13}b\text{)}$$

Further details of the solution may be found in Bush & Fendell (1973*a*). Results of a numerical computation carried out with the parameter values given in (A 12) are presented in figures 2, 5 and 6; of course, the parameter a does not enter the self-similar solution to the modified case.

Appendix B. The transient counterflow case

Formulation

The second flow case to be considered is the transient counterflow case, for which the flow quantities are taken to be

$$\left.\begin{aligned} u(x,y,t) = xU(y,t) \quad v(x,y,t) = V(y,t), \quad p(x,y,t) = P(y,t) + \tfrac{1}{2}x^2P^+(t), \\ T(x,y,t) = H(y,t), \quad Y_i(x,y,t) = J_i(y,t), \quad \Phi_q(x,y,t) = F_q(y,t). \end{aligned}\right\} \quad \text{(B 1)}$$

For this case, then, the governing equations are

$$\frac{\partial}{\partial t}\left(\frac{1}{H}\right)+\frac{U}{H}+\frac{\partial}{\partial y}\left(\frac{V}{H}\right)=0, \tag{B 2a}$$

$$\frac{1}{H}\left(\frac{\partial U}{\partial t}+U^2+V\frac{\partial U}{\partial y}\right)+P^+-\frac{\partial}{\partial y}\left(H\frac{\partial U}{\partial y}\right)=0, \tag{B 2b}$$

$$\frac{1}{H}\left(\frac{\partial V}{\partial t}+V\frac{\partial V}{\partial y}\right)+\frac{\partial P}{\partial y}-(2+m)\frac{\partial}{\partial y}\left(H\frac{\partial V}{\partial y}\right)-m\frac{\partial}{\partial y}(HU)-H\frac{\partial U}{\partial y}=0, \tag{B 2c}$$

$$\frac{1}{H}\left(\frac{\partial F_q}{\partial t}+V\frac{\partial F_q}{\partial y}\right)-\frac{\partial}{\partial y}\left(H\frac{\partial F_q}{\partial y}\right)=0. \tag{B 2d}$$

Associated with (B 2) are the boundary conditions ($\hat{F}(t)=F(+\infty,t)$ and $\check{F}(t)=F(-\infty,t)$)

$$\left.\begin{aligned}\hat{U},\hat{H}&=\text{specified functions of } t, \quad \text{with } \frac{1}{\hat{H}}\left(\frac{d\hat{U}}{dt}+\hat{U}^2\right)=-P^+,\\ \hat{J}_B,\hat{J}_{B_2}&=\text{specified function of } t, \quad \hat{J}_A,\hat{J}_{A_2},\hat{J}_{C_{(1)}},\hat{J}_{C_{(2)}}=0,\end{aligned}\right\} \tag{B 3a}$$

$$\left.\begin{aligned}\check{U},\check{H}&=\text{specified functions of } t, \quad \text{with } \frac{1}{\check{H}}\left(\frac{d\check{U}}{dt}+\check{U}^2\right)=-P^+,\\ \check{J}_A,\check{J}_{A_2}&=\text{specified functions of } t, \quad \check{J}_B,\check{J}_B,\check{J}_{C_{(1)}},\check{J}_{C_{(2)}}=0.\end{aligned}\right\} \tag{B 3b}$$

Here, as in § 3, it is assumed that only species B and/or B_2 exist as $y\to+\infty$, while only species A and/or A_2 exist as $y\to-\infty$.

Consider now the particular case where

$$U(y,t)=\hat{U}(t)=\check{U}(t)=1/(t_0+t), \quad \text{with} \quad t_0=\text{reference constant}. \tag{B 4}$$

For this case, from (B 3), it is seen that $P^+(t)=0$, and thus (B 2b) becomes an identity.

Application of a modified Howarth–Dorodnitsyn transformation (different from the one employed in § 3) $(y,t)\to(\xi,\eta)$, with

$$\xi=\tfrac{3}{4}\log\left\{\frac{(t_0+t)}{t_0}\right\}, \quad \eta=\left\{\frac{3}{4}\frac{1}{(t_0+t)}\right\}^{\frac{1}{2}}\int_0^y\frac{dz}{H}, \tag{B 5a}$$

to (B 2a) yields

$$V'=-2\eta H'+\frac{\partial}{\partial\xi}\left(\int_0^\eta H'\,d\chi\right)+\frac{2}{3}\left(\int_0^\eta H'\,d\chi\right), \tag{B 5b}$$

with $V'(\xi,\eta)=\{\frac{4}{3}(t_0-t)\}^{\frac{1}{2}}V(y,t)$ and $H'(\xi,\eta)=H(y,t)$. Under this transformation, then, it is seen from (B 2d) that the functions $F'_q(\xi,\eta)=F_q(y,t)$ satisfy, in the domain $\xi>0$, $-\infty<\eta<+\infty$,

$$\frac{\partial^2F'_q}{\partial\eta^2}+2\eta\frac{\partial F'_q}{\partial\eta}-\frac{\partial F'_q}{\partial\xi}=0. \tag{B 6a}$$

Note that, with the introduction of the operator L', defined by

$$L'\{F'(\xi,\eta)\}=\left\{\frac{\partial^2}{\partial\eta^2}+2\eta\frac{\partial}{\partial\eta}-\frac{\partial}{\partial\xi}\right\}\{F'(\xi,\eta)\}, \tag{B 7}$$

the equations for the Shvab–Zeldovich functions may be expressed as

$$L'\{F'_q\} = 0. \tag{B 6b}$$

Further, to the order of approximation considered, the components of the functions $F'_q(\xi,\eta)$, namely, $H'(\xi,\eta) = H(y,t)$ and $J'_i(\xi,\eta) = J_i(y,t)$, satisfy

$$L'\{H'\} = -(Q'_1\,\Omega'_1\,G'_1 + Q'_2\,\Omega'_2\,G'_2), \tag{B 8a}$$

$$L'\{J'_A\} = \Omega'_1\,G'_1 - \Omega'_2\,G'_2, \quad L'\{J'_{A_2}\} = \Omega'_2\,G'_2, \tag{B 8b}$$

$$L'\{J'_B\} = \Omega'_2\,G'_2 - \Omega'_1\,G'_1, \quad L'\{J'_{B_2}\} = \Omega'_1\,G'_1, \tag{B 8c}$$

$$L'\{J'_{C_{(1)}}\} = -\Omega'_1\,G'_1, \quad L'\{J'_{C_{(2)}}\} = -\Omega'_2\,G'_2, \tag{B 8d}$$

where the quantities $G'_k(\xi,\eta)$ are given by

$$G'_1 = \tfrac{4}{3}t_0 \exp\{-\theta'_1(T'^*_1 - H')/H'\}\,J'_A\,J'_{B_2}\exp\{\tfrac{4}{3}\xi\}, \tag{B 9a}$$

$$G'_2 = \tfrac{4}{3}t_0 \exp\{-\theta'_2(T'^*_2 - H')/H'\}\,J'_B\,J'_{A_2}\exp\{\tfrac{4}{3}\xi\}. \tag{B 9b}$$

From (B 3), it is seen that the system of equations (B 6) and/or (B 8) must satisfy

$$H' \to \hat{H}, \quad J'_B \to \hat{J}_B, \quad J'_{B_2} \to \hat{J}_{B_2}, \quad J'_A, J'_{A_2}, J'_{C_{(1)}}, J'_{C_{(2)}} \to 0 \quad \text{as} \quad \eta \to +\infty, \tag{B 10a}$$

$$H' \to \check{H}, \quad J'_A \to \check{J}_A, \quad J'_{A_2} \to \check{J}_{A_2}, \quad J'_B, J'_{B_2}, J'_{C_{(1)}}, J'_{C_{(2)}} \to 0 \quad \text{as} \quad \eta \to -\infty. \tag{B 10b}$$

For what follows, it is assumed that $\hat{H}$, $\hat{J}_B$, $\hat{J}_{B_2}$, $\check{H}$, $\check{J}_A$ and $\check{J}_{A_2}$ are specified constants.

Near-equilibrium flame structure: parameter expansion analysis

Attention is directed now to the determination of the solutions for the flow quantities $F'(\xi,\eta)$ ($= H'(\xi,\eta)$, $J'_i(\xi,\eta)$ and/or $F'_q(\xi,\eta)$) in the near-equilibrium limit, defined by

$$\Omega'_k = Z'_k \exp\{-\theta'_k\} \equiv \nu'_k\,\Omega = \{\tfrac{4}{3}t_0\}^{-1}\nu_k\,\Omega \to \infty, \tag{B 11a}$$

for the case where

$$\theta'_k = \vartheta_k\,\theta = O(1). \tag{B 11b}$$

Specifically, it is assumed that $\Omega \to \infty$ and $\theta = O(1)$, with ν_k (and ν'_k) and $\vartheta_k = O(1)$.

First, solutions for the variables $F'(\xi,\eta)$, in the near-equilibrium limit $\Omega \to \infty$ with $\theta = O(1)$, are sought in terms of outer asymptotic expansions of the form

$$F'(\xi,\eta) \cong \sum_{s=0} \Delta^{(s)}(\Omega)\,F^{(s)}(\xi,\eta) = F^{(0)}(\xi,\eta) + \Delta^{(1)}(\Omega)\,F^{(1)}(\xi,\eta) + \ldots. \tag{B 12}$$

Here, it is assumed that $\Delta^{(0)}(\Omega) = 1$ and $\Delta^{(s+1)}(\Omega)/\Delta^{(s)}(\Omega) \to 0$ as $\Omega \to \infty$, while $F^{(s)}(\xi,\eta) = O(1)$ for $\xi,\eta = O(1)$. Solutions based on these expansions should be valid except, possibly, near $\eta_k(\xi)$, the locations of the reaction fronts. Application of this expansion scheme to the Shvab–Zeldovich functions $F'_q(\xi,\eta)$ yields, to leading order of approximation,

$$\left.\begin{aligned} &F_q^{(0)}(\xi,\eta) = F_q^{(0)}(\eta), \quad \text{so that} \quad \frac{d^2F_q^{(0)}}{d\eta^2} + 2\eta\frac{dF_q^{(0)}}{d\eta} = 0, \\ &F_q^{(0)} \to \hat{F}_q = \text{constant} \quad \text{as} \quad \eta \to +\infty, \qquad F_q^{(0)} \to \check{F}_q = \text{constant} \quad \text{as} \quad \eta \to -\infty. \end{aligned}\right\} \tag{B 13a}$$

Then, the solutions of the above boundary-value problems are given by

$$\left.\begin{aligned} F_q^{(0)}(\eta) &= \tfrac{1}{2}[\hat{F}_q\{1+\operatorname{erf}\eta\}+\check{F}_q\{1-\operatorname{erf}\eta\}] \\ &= a_q^{(0)}\operatorname{erf}\eta + b_q^{(0)}, \end{aligned}\right\} \qquad \text{(B 13}b\text{)}$$

with $$a_q^{(0)} = \tfrac{1}{2}(\hat{F}_q - \check{F}_q), \quad b_q^{(0)} = \tfrac{1}{2}(\hat{F}_q + \check{F}_q). \Big\}$$

From the definitions of the Shvab–Zeldovich functions [cf. (2.6)], it follows that, for example,

$$a_T^{(0)} = \tfrac{1}{2}\{(\hat{H}+Q_1'\hat{J}_{B_2})-(\check{H}+Q_2'\check{J}_{A_2})\}, \quad b_T^{(0)} = \tfrac{1}{2}\{(\hat{H}+Q_1'\hat{J}_{B_2})+(\check{H}+Q_2'\check{J}_{A_2})\}, \qquad \text{(B 14}a\text{)}$$

$$\left.\begin{aligned} a_A^{(0)} &= -\tfrac{1}{2}(\check{J}_A+\check{J}_{A_2}+\hat{J}_{B_2}), \quad b_A^{(0)} = \tfrac{1}{2}(\check{J}_A+\check{J}_{A_2}-\hat{J}_{B_2}), \\ a_B^{(0)} &= \tfrac{1}{2}(\hat{J}_B+\hat{J}_{B_2}+\check{J}_{A_2}), \quad b_B^{(0)} = \tfrac{1}{2}(\hat{J}_B+\hat{J}_{B_2}-\check{J}_{A_2}). \end{aligned}\right\} \qquad \text{(B 14}b\text{)}$$

Here, it is assumed that $Q_k' = O(1)$.

To the order of approximation considered, from the Burke–Schumann thin-flame model (cf. § 3), at the equilibrium flame fronts, $\eta \to \eta_1(\xi) \cong \eta_1^{(0)} =$ constant and $\eta \to \eta_2(\xi) \cong \eta_2^{(0)} =$ constant, respectively, and $J_A^{(0)}, J_{B_2}^{(0)}, J_B^{(0)}, J_{A_2}^{(0)} \to 0$. Further from the very nature of the two-step chain reaction itself, it is necessary that $J_{A_2}^{(0)} \to 0$ as $\eta \to \eta_1^{(0)}$ and that $J_{B_2}^{(0)} \to 0$ as $\eta \to \eta_2^{(0)}$. Thus, the positions of the two (thin) flames are determined as follows:

$$F_A^{(0)}(\eta_1^{(0)}) = 0 \quad \text{so that} \quad \operatorname{erf}\eta_1^{(0)} = -b_A^{(0)}/a_A^{(0)} = (\check{J}_A+\check{J}_{A_2}-\hat{J}_{B_2})/(\check{J}_A+\check{J}_{A_2}+\hat{J}_{B_2}); \qquad \text{(B 15}a\text{)}$$

$$F_B^{(0)}(\eta_2^{(0)}) = 0, \quad \text{so that} \quad \operatorname{erf}\eta_2^{(0)} = -b_B^{(0)}/a_B^{(0)} = -(\hat{J}_B+\hat{J}_{B_2}-\check{J}_{A_2})/(\hat{J}_B+\hat{J}_{B_2}+\check{J}_{A_2}). \qquad \text{(B 15}b\text{)}$$

From these equations it follows that $\eta_1^{(0)} - \eta_2^{(0)} \geqslant 0$, since

$$\operatorname{erf}\eta_1^{(0)} - \operatorname{erf}\eta_2^{(0)} = b_B^{(0)}/a_B^{(0)} - b_A^{(0)}/a_A^{(0)} = \check{J}_A(\hat{J}_B+2\hat{J}_{B_2})+\hat{J}_B(\check{J}_A+2\check{J}_{A_2}) \geqslant 0. \qquad \text{(B 16)}$$

It is noted that $\eta_1^{(0)} - \eta_2^{(0)} \to 0$ if *both* $\check{J}_A$ and $\hat{J}_B \to 0$. The reference flame temperatures $T_k'^*$, introduced in (B 9), are now (conveniently) identified to be the values attained by $H^{(0)}$ at $\eta_k^{(0)}$, i.e.,

$$\begin{aligned} F_T^{(0)}(\eta_1^{(0)}) &= H^{(0)}(\eta_1^{(0)}) \\ &= a_T^{(0)}\operatorname{erf}(\eta_1^{(0)}) + b_T^{(0)} = (a_A^{(0)}b_T^{(0)} - b_A^{(0)}a_T^{(0)})/a_A^{(0)} = T_1'^*, \qquad \text{(B 17}a\text{)} \\ F_T^{(0)}(\eta_2^{(0)}) &= H^{(0)}(\eta_2^{(0)}) \\ &= a_T^{(0)}\operatorname{erf}(\eta_2^{(0)}) + b_T^{(0)} = (a_B^{(0)}b_T^{(0)} - b_B^{(0)}a_T^{(0)})/a_B^{(0)} = T_2'^*. \qquad \text{(B 17}b\text{)} \end{aligned}$$

The magnitudes of the finite reactant mass fractions at the respective flames are

$$\begin{aligned} F_B^{(0)}(\eta_1^{(0)}) &= J_B^{(0)}(\eta_1^{(0)}) \\ &= a_B^{(0)}\operatorname{erf}(\eta_1^{(0)}) + b_B^{(0)} = (a_A^{(0)}b_B^{(0)} - b_A^{(0)}a_B^{(0)})/a_A^{(0)} = J_{B,1}'^*, \qquad \text{(B 18}a\text{)} \\ F_A^{(0)}(\eta_2^{(0)}) &= J_A^{(0)}(\eta_2^{(0)}) \\ &= a_A^{(0)}\operatorname{erf}(\eta_2^{(0)}) + b_B^{(0)} = (a_B^{(0)}b_A^{(0)} - b_B^{(0)}a_A^{(0)})/a_B^{(0)} = J_{A,2}'^*. \qquad \text{(B 18}b\text{)} \end{aligned}$$

It is noted that, if $\check{J}_A$ and $\hat{J}_B \to 0$ (such that $(\eta_1^{(0)} - \eta_2^{(0)}) \to 0$), then $J_{A,2}'^*$ and $J_{B,1}'^* \to 0$.

Thus, the thin-flame (or leading-order outer expansion) solutions are summarized by

$$J_A^{(0)}, J_{A_2}^{(0)} = 0, \quad J_B^{(0)} = F_A^{(0)} + F_B^{(0)}, \quad J_{B_2}^{(0)} = -F_A^{(0)}, \quad H^{(0)} = F_T^{(0)} + Q_1' F_A^{(0)} \quad \text{in} \quad \eta_1^{(0)} < \eta < \infty; \tag{B 19a}$$

$$J_{A_2}^{(0)}, J_{B_2}^{(0)} = 0, \quad J_A^{(0)} = F_A^{(0)}, \quad J_B^{(0)} = F_B^{(0)}, \quad H^{(0)} = F_T^{(0)} \quad \text{in} \quad \eta_2^{(0)} < \eta < \eta_1^{(0)}; \tag{B 19b}$$

$$J_B^{(0)}, J_{B_2}^{(0)} = 0, \quad J_A^{(0)} = F_A^{(0)} + F_B^{(0)}, \quad J_{A_2}^{(0)} = -F_B^{(0)}, \quad H^{(0)} = F_T^{(0)} + Q_2' F_B^{(0)} \quad \text{in} \quad -\infty < \eta < \eta_2^{(0)}. \tag{B 19c}$$

To complete the presentation of the outer expansion solutions, it is noted that, since

$$\operatorname{erf}\eta \to \operatorname{erf}\eta_k^{(0)} + 2\pi^{-\frac{1}{2}} \exp\{-(\eta_k^{(0)})^2\}(\eta - \eta_k^{(0)}) + \ldots \quad \text{as} \quad \eta \to \eta_k^{(0)},$$

as $\eta \to \eta_1^{(0)}$

$$\left.\begin{aligned} F_T^{(0)} &\to T_1'^* + [2\pi^{-\frac{1}{2}} a_T^{(0)} \exp\{-(\eta_1^{(0)})^2\}](\eta - \eta_1^{(0)}) + \ldots \\ &= T_1'^* + \beta_{T,1}(\eta - \eta_1^{(0)}) + \ldots, \\ F_B^{(0)} &\to J_{B,1}'^* + [2\pi^{-\frac{1}{2}} a_B^{(0)} \exp\{-(\eta_1^{(0)})^2\}](\eta - \eta_1^{(0)}) + \ldots \\ &= J_{B,1}'^* + \beta_{B,1}(\eta - \eta_1^{(0)}) + \ldots, \\ F_A^{(0)} &\to [2\pi^{-\frac{1}{2}} a_A^{(0)} \exp\{-(\eta_1^{(0)})^2\}](\eta - \eta_1^{(0)}) + \ldots \\ &= \beta_{A,1}(\eta - \eta_1^{(0)}) + \ldots; \end{aligned}\right\} \tag{B 20a}$$

while as $\eta \to \eta_2^{(0)}$

$$\left.\begin{aligned} F_T^{(0)} &\to T_2'^* + [2\pi^{-\frac{1}{2}} a_T^{(0)} \exp\{-(\eta_1^{(0)})^2\}](\eta - \eta_2^{(0)}) + \ldots \\ &= T_2'^* + \beta_{T,2}(\eta - \eta_2^{(0)}) + \ldots, \\ F_A^{(0)} &\to J_{A,2}'^* + [2\pi^{-\frac{1}{2}} a_A^{(0)} \exp\{-(\eta_2^{(0)})^2\}](\eta - \eta_2^{(0)}) + \ldots \\ &= J_{A,2}'^* + \beta_{A,2}(\eta - \eta_2^{(0)}) + \ldots, \\ F_B^{(0)} &\to [2\pi^{-\frac{1}{2}} a_B^{(0)} \exp\{-(\eta_2^{(0)})^2\}](\eta - \eta_2^{(0)}) + \ldots \\ &= \beta_{B,2}(\eta - \eta_2^{(0)}) + \ldots. \end{aligned}\right\} \tag{B 20b}$$

For examination of the behaviour of the flow quantities near the flame fronts in greater detail, the following ('stretched') spatial co-ordinates are introduced:

$$\zeta_k = (\eta - \eta_k^{(0)})/\delta_k(\Omega), \quad \text{with} \quad \delta_k \to 0 \quad \text{as} \quad \Omega \to \infty. \tag{B 21a}$$

Solutions for the variables $F'(\xi, \eta)$, in the limit $\Omega \to \infty$ with $\theta = O(1)$, are now sought in terms of inner expansions of the form

$$F'(\xi, \eta) \cong \sum_{r=0} \Gamma_k^{(r)}(\Omega) H_k^{(r)}(\xi, \zeta_k) = \Gamma_k^{(0)}(\Omega) H_k^{(0)}(\xi, \zeta_k) + \Gamma_k^{(1)}(\Omega) H_k^{(1)}(\xi, \zeta_k) + \ldots, \tag{B 21b}$$

with $\Gamma_k^{(r+1)}(\Omega)/\Gamma_k^{(r)}(\Omega) \to 0$ as $\Omega \to \infty$, and $H_k^{(r)}(\xi, \zeta_k) = O(1)$ for $\xi, \zeta_k = O(1)$. For the sake of brevity, only the analysis for $k = 1$ is presented here; the parallel analysis for $k = 2$ follows directly.

Application of the present expansion scheme to the Shvab–Zeldovich functions $F'_T(\xi,\eta)$, $F'_B(\xi,\eta)$ and $F'_A(\xi,\eta)$ yields [cf. (B 20a)], to the leading orders of approximation,

$$\left.\begin{aligned} F'_T \cong T'^*_1 + \delta_1\beta_{T,1}\zeta_1 + \ldots, \quad F'_B \cong J'^*_{B,1} + \delta_1\beta_{B,1}\zeta_1 + \ldots, \\ F'_A \cong \delta_1\beta_{A,1}\zeta_1 + \ldots. \end{aligned}\right\} \tag{B 22}$$

The solutions of (B 22) *suggest* that the inner expansions for the components of the Shvab–Zeldovich functions should reduce to the following forms:

$$H'(\xi,\eta) \cong T'^*_1 + \delta_1(\Omega)\, h_{T,1}(\xi,\zeta_1) + \ldots; \tag{B 23a}$$

$$\left.\begin{aligned} J'_B(\xi,\eta) \cong J'^*_{B,1} + \delta_1(\Omega) j_{B,1}(\xi,\zeta_1) + \ldots, \\ J'_{B_2}(\xi,\eta) \cong \delta_1(\Omega) j_{B_2,1}(\xi,\zeta_1) + \ldots; \end{aligned}\right\} \tag{B 23b}$$

$$\left.\begin{aligned} J'_A(\xi,\eta) \cong \delta_1(\Omega) j_{A,1}(\xi,\zeta_1) + \ldots, \\ J'_{A_2}(\xi,\eta) \cong \delta_1(\Omega)\, \sigma_{A_2,1}(\Omega) j_{A_2,1}(\xi,\zeta_1) + \ldots, \end{aligned}\right\} \tag{B 23c}$$

where it is assumed that $\sigma_{A_2,1}(\Omega) \to 0$ as $\Omega \to \infty$. Substitution of these expansions into the equations describing the Shvab–Zeldovich functions gives

$$\left.\begin{aligned} h_{T,1} + Q'_1 j_{B_2,1} = \beta_{T,1}\zeta_1, \quad j_{B,1} + j_{B_2,1} = \beta_{B,1}\zeta_1, \\ j_{A,1} - j_{B_2,1} = \beta_{A,1}\zeta_1. \end{aligned}\right\} \tag{B 24a}$$

Equation (B 24a) furnishes three equations for the four unknowns $h_{T,1}$, $j_{B,1}$, $j_{B_2,1}$ and $j_{A,1}$; a fourth equation is derivable from the second equation of (B 8c). Application of the inner expansion scheme to this equation yields

$$\partial^2 j_{B_2,1}/\partial\zeta_1^2 = j_{A,1} j_{B_2,1} \exp\{\tfrac{4}{3}\xi\}. \tag{B 24b}$$

Here, the following identification has been made:

$$\delta_1(\Omega) = (\nu_1\Omega)^{-\frac{1}{3}} \to 0 \quad \text{as} \quad \Omega \to \infty. \tag{B 25}$$

From (B 24), the following equation for $j_{B_2,1}(\xi,\zeta_1)$ is derived:

$$\partial^2 j_{B_2,1}/\partial\zeta_1^2 = (\beta_{A,1}\zeta_1 + j_{B_2,1}) j_{B_2,1} \exp\{\tfrac{4}{3}\xi\}, \tag{B 26a}$$

with $\beta_{A,1} < 0$ [cf. (B 14b) and (B 20a)]. Alternatively, by the change of variables

$$\chi = (-\beta_{A,1})^{\frac{1}{3}} \exp\{\tfrac{4}{9}\xi\}\zeta_1, \quad \Psi = (-\beta_{A,1})^{-\frac{2}{3}} \exp\{\tfrac{4}{9}\xi\} j_{B_2,1} \tag{B 27}$$

(B 26) is brought into the 'universal form'

$$\partial^2\Psi/\partial\chi^2 = (\Psi - \chi)\Psi. \tag{B 26b}$$

The boundary conditions associated with (B 26) are

$$j_{B_2,1} \to (-\beta_{A,1})\zeta_1 \to +\infty \quad \text{as} \quad \zeta_1 \to +\infty \quad \text{and/or} \quad \Psi \to \chi \to +\infty \quad \text{as} \quad \chi \to +\infty; \tag{B 28a}$$

$$j_{B_2,1} \to 0 \quad \text{as} \quad \zeta_1 \to -\infty \quad \text{and/or} \quad \Psi \to 0 \quad \text{as} \quad \chi \to -\infty. \tag{B 28b}$$

Further, it should be noted that, for $\chi \to -\infty$ with $\Psi \to \mathring{\Psi} \to 0$, (B 26$b$) yields

$$\partial^2\mathring{\Psi}/\partial\chi^2 \to -\chi\mathring{\Psi}, \quad \text{so that} \quad \mathring{\Psi} \sim \exp\{-\tfrac{2}{3}(-\chi)^{\frac{3}{2}}\}; \tag{B 29a}$$

while for $\chi \to +\infty$ with $\Psi \to \chi + \hat{\Psi} \to \chi$, (B 26*b*) yields

$$\partial^2\hat{\Psi}/\partial\chi^2 \to \chi\hat{\Psi}, \quad \text{so that} \quad \hat{\Psi} \sim \exp\{-\tfrac{2}{3}\chi^{\frac{3}{2}}\}. \tag{B 29b}$$

From the above, it is seen that only an exponentially small amount of reactant penetrates the near-equilibrium flame for the second-order reaction under study.

Thus, the flame structure (or leading-order inner expansion) solutions for reaction 1 are summarized, in terms of the variables of (B 27), by

$$\left.\begin{aligned} j_{B_2,1} &= (-\beta_{A,1})^{\frac{3}{2}} \exp\{-\tfrac{4}{9}\xi\}\Psi, \\ j_{A,1} &= (-\beta_{A,1})^{\frac{3}{2}} \exp\{-\tfrac{4}{9}\xi\}(\Psi - \chi), \end{aligned}\right\} \tag{B 30a}$$

$$j_{B,1} = \{\beta_{B,1}/(-\beta_{A,1})^{\frac{1}{2}}\} \exp\{-\tfrac{4}{9}\xi\}(\chi - \{-\beta_{A,1}/\beta_{B,1}\}\Psi), \tag{B 30b}$$

$$h_{T,1} = \{\beta_{T,1}/(-\beta_{A,1})^{\frac{1}{2}}\} \exp\{-\tfrac{4}{9}\xi\}(\chi - Q_1'\{-\beta_{A,1}/\beta_{T,1}\}\Psi). \tag{B 30c}$$

It is noted that the thickness of the flame zone is $O(\Omega'^{-\frac{1}{3}})$, and the magnitude of the deviation of the temperature in this flame zone from $T_1'^*$ is also $O(\Omega'^{-\frac{1}{3}})$, where it is taken that $\Omega_1' \to \infty$. With respect to this scaling for the thickness and temperature deviation, it is seen, from a basic low-speed deflagration formulation (cf. footnote on p. 704), that, in order for the inner expansions to be self-consistent, it is required that $\Pi'\Omega'^{\frac{1}{3}} \to 0$.

Near-equilibrium flame structure: co-ordinate expansion analysis

Consider the flow problem formulated in terms of the independent variables τ and η, rather than ξ and η, with τ and η given by [cf. (B 5) and (B 11)]

$$\tau = \Omega \exp\{\tfrac{4}{3}\xi\} = \Omega \frac{(t_0+t)}{t_0}, \quad \eta = \frac{\sqrt{3}}{2} \frac{1}{(t_0+t)^{\frac{1}{2}}} \int_0^y \frac{dz}{H}. \tag{B 31}$$

Solutions are sought in the spatial domain $-\infty < \eta < +\infty$ in the limit $\tau \to \infty$ (cf., for example, Krishnamurthy & Williams 1971; Bush & Fendell 1973*a*), where $\tau \to \infty$ is identified as a singular near-equilibrium limit.

Two properties of the solution seem noteworthy. First, one may write, for the co-ordinate expansion analysis, the inner variables ζ_k as

$$\zeta_k \sim (\tfrac{3}{4})^{\frac{1}{2}} \left(\frac{\nu_k}{t_0}\right)^{\frac{1}{3}} \frac{\Omega^{\frac{1}{3}}}{T_k'^*} \frac{y - y_k}{(t_0+t)^{\frac{1}{6}}} \sim \Omega^{\frac{1}{3}} \frac{(y-y_k)}{t^{\frac{1}{6}}} \quad \text{as} \quad t \to \infty; \tag{B 32a}$$

while, within the flame zones, the deviations of the temperatures (say) from their thin-flame (or equilibrium) values are given by

$$T_k'^* - H' \sim \eta - \eta_k^{(0)} \sim (\tfrac{3}{4})^{\frac{1}{2}} \frac{1}{T_k'^*} \frac{y - y_k}{(t_0+t)^{\frac{1}{2}}} \sim \frac{y-y_k}{t^{\frac{1}{2}}} \quad \text{as} \quad t \to \infty. \tag{B 32b}$$

While the departure of the temperature from the adiabatic flame temperature goes to zero as $t^{-\frac{1}{2}}$ (for $t \to \infty$) within the flame zones (to the leading order of approximation), the spatial thickness of the domain of the inner expansion increases as $t^{\frac{1}{6}}$, all parameters being held constant.

Second, the magnitude of the fuel consumption per unit time (the so-called

'apparent flame strength') is conveniently characterized by, for the flame near $y^\dagger = y_1^\dagger$,

$$\dot{m}_1^\dagger = (\rho_r^\dagger k_r^\dagger \mu_r^\dagger)^{\frac{1}{2}} \left| -T' \frac{\partial Y'_{B_2}}{\partial y'} \right|_{y'=y'_1}$$

$$\cong (\rho_r^\dagger k_r^\dagger \mu_r^\dagger)^{\frac{1}{2}} \left| -H \frac{\partial J_{B_2}}{\partial y} \right|_{y=y_1} + \ldots, \qquad \text{(B 33}a\text{)}$$

where quantities with a dagger superscript are dimensional, while those with subscript r are representative values. For the co-ordinate expansion analysis, by (B 31),

$$\frac{\dot{m}_1^\dagger}{(\rho_r^\dagger \mu_r^\dagger k_r^\dagger)^{\frac{1}{2}}} \cong \{\tfrac{4}{3} t_0\}^{-\frac{1}{2}} \frac{\Omega^{\frac{1}{2}}}{\tau^{\frac{1}{2}}} \left| -\frac{\partial J'_{B_2}}{\partial \eta} \right|_{\eta=\eta_1} + \ldots, \qquad \text{(B 33}b\text{)}$$

while, for the parameter expansion analysis by (B 5a),

$$\frac{\dot{m}_1^\dagger}{(\rho_r^\dagger \mu_r^\dagger k_r^\dagger)^{\frac{1}{2}}} \cong \{\tfrac{4}{3} t_0\}^{-\frac{1}{2}} \exp\{-\tfrac{2}{3}\xi\} \left| -\frac{\partial J'_{B_2}}{\partial \eta} \right|_{\eta=\eta_1} + \ldots . \qquad \text{(B 33}c\text{)}$$

For chemical equilibrium the expressions on the right-hand side of (B 33b) and (B 33c) are independent of $k_r^\dagger$, so $\dot{m}^\dagger \sim (k_r^\dagger)^{\frac{1}{2}}$, all other parameters being held constant. Statements entirely analogous to (B 33b) and (B 33c) hold for the reactant consumption rate at the other flame at $\eta = \eta_2$, except that the gradient factor involves J'_{A_2} rather than J'_{B_2}.

REFERENCES

Brown, G. & Roshko, A. 1971 The effect of density difference on the turbulent mixing layer. In *Turbulent Shear Flow, AGARD Conf. Proc.* no. 93, pp. 23-1–23-12.

Burke, S. P. & Schumann, T. E. W. 1928 Diffusion flames. *Indust. Engng Chem.* **20**, 998–1004.

Bush, W. B. & Fendell, F. E. 1973*a* The structure of multiple diffusion flames for a two-step chain reaction. *Project SQUID Tech. Rep.* TRW-6-PU. Purdue University.

Bush, W. B. & Fendell, F. E. 1973*b* On duffusion flames in turbulent shear flows. *Project SQUID Tech. Rep.* TRW-7-PU. Purdue University. (To appear in *Acta Astronautica*.)

Carslaw, H. S. & Jaeger, J. C. 1959 *Conduction of Heat in Solids*. 2nd edn, p. 53. Oxford: Clarendon Press.

Clarke, J. F. 1968 On the structure of a hydrogen–oxygen diffusion flame. *Proc. Roy. Soc.* A **307**, 283–302.

Clarke, J. F. 1969 Reaction-broadening in a hydrogen–oxygen diffusion flame. *Proc. Roy. Soc.* A **312**, 65–83.

Clarke, J. F. & Moss, J. B. 1969 The effect of the large hydrogen-dissociation activation energy on an equilibrium-broadened hydrogen–oxygen diffusion flame. *Proc. Roy. Soc.* A **313**, 433–443.

Cohen, C. B., Bromberg, R. & Lipkis, R. P. 1958 Boundary layers with chemical reactions due to mass addition. *Jet Propulsion*, **28**, 659–668.

Edelman, R. B., Fortune, O. & Weilerstein, G. 1972 Analytic study of gravity effects in laminar diffusion flames. *Gen. Appl. Sci. Lab. Rep.* TR-771. New York: Westbury.

Fendell, F. E. 1965 Ignition and extinction in combustion of initially unmixed reactants. *J. Fluid Mech.* **21**, 281–303.

Fendell, F. E. 1967 Flame structure in initially unmixed reactants under one-step kinetics. *Chem. Engng Sci.* **22**, 1829–1837.

FRIEDLANDER, S. K. & KELLER, K. H. 1963 The structure of the zone of diffusion controlled reaction. *Chem. Engng Sci.* **18**, 365–375.

GIBSON, C. H. & LIBBY, P. A. 1972 On turbulent flows with fast chemical reaction. Part 2. The distribution of reactants and products near a reacting surface. *Combustion Sci. Tech.* **6**, 29–35.

GRANT, A. J., JONES, J. M. & ROSENFELD, J. L. J. 1973 Orderly structure and unmixedness in lifted jet diffusion flames. *Thorton Res. Centre Rep.* Chester, England: Shell Research Ltd.

GUREVICH, M. A. & STEPANOV, A. M. 1973 Diffusion burning of a liquid-fuel drop in a two-oxidizer mixture. *Combustion, Explosion & Shock Waves*, **6**, 218–220. [Trans. from *Fiz. Goreniya i Vzryva* **6** (1970), 243–245.]

HAWTHORNE, W. R., WEDDELL, D. S. & HOTTEL, H. C. 1949 Mixing and combustion in turbulent gas jets. *3rd Symposium on Combustion and Flame and Explosion Phenomena*, pp. 266–288. Baltimore: Williams & Wilkins.

KERBER, R. L., EMANUEL, G. & WHITTIER, J. S. 1972 Computer modelling and parametric study for a pulsed H_2+F_2 laser. *Appl. Optics*, **11**, 1112–1123.

KLIMOV, A. M. 1967 On the mechanism of turbulent burning. *Theory and Practice of Gas Burning*, pp. 167–172. Leningrad: Nedra. (In Russian.)

KORMAN, H. F. 1970 Theoretical modelling of cool flames. *Combustion Sci. Tech.* **2**, 149–519.

KRISHNAMURTHY, L. & WILLIAMS, F. A. 1971 Kinetics and regression. *SIAM J. Appl. Math.* **20**, 590–611.

LIÑAN, A. 1963 On the structure of laminar diffusion flames. Aero. Engng thesis, California Institute of Technology, Pasadena.

OTSUKA, Y. & NIIOKA, T. 1972 On the deviation of the flame from the stagnation point in opposed-jet diffusion flames. *Combustion & Flame*, **19**, 171–179.

OTSUKA, Y. & NIIOKA, T. 1973 The one-dimensional diffusion flame in a two-dimensional counter-flow burner. *Combustion & Flame*, **21**, 163–176.

PEARSON, J. R. A. 1963 Diffusion of one substance into a semi-infinite medium containing another with second-order reaction. *Appl. Sci. Res.* A **11**, 321–340.

SCHETZ, J. A. 1970 A simplified model for combustion of multicomponent fuels in air. *Combustion & Flame*, **15**, 57–60.

STEWARTSON, K. 1964 *The Theory of Laminar Boundary Layers in Compressible Fluids*, chap. 6. Oxford University Press.

TSUJI, H. & YAMAOKA, I. 1971 Structure analysis of counterflow diffusion flames in the forward stagnation region of a porous cylinder. *13th Symp. (Int.) on Combustion*, pp. 723–731. Pittsburgh: Combustion Institute.

WILLIAMS, F. A. 1965 *Combustion Theory*, chaps 1 and 3. Addison-Wesley.

ZELDOVICH, J. 1946 The oxidation of nitrogen in combustion and explosives. *Acta Physiocochemica U.S.S.R.* **21**, 577–628.